Measurement of the Dispersion Relation for Rayleigh Surface Phonons of LiF(001) by Inelastic Scattering of He Atoms

G. Brusdeylins, R. Bruce Doak, and J. Peter Toennies
Max Planck Institut für Strömungsforschung, D-3400 Göttingen, Federal Republic of Germany
(Received 27 October 1980)

Time-of-flight spectra of low-energy (≈ 20 meV) He scattered from a LiF(001) crystal along the ⟨100⟩ direction reveal up to five sharp inelastic-scattering maxima. Their scattering angle and flight time determine the frequencies and wave numbers of surface phonons over the entire Brillouin zone. The results agree well with calculations of Rayleigh modes by de Wette and Benedek except near the zone boundary. Further unidentified features are also observed.

PACS numbers: 68.30.+z, 63.20.Dj

Surface phonons play a vital role in understanding heterogeneous catalysis, surface phase transitions, and almost all areas of surface physics. They are also involved in many technical applications, such as heat transmission through interfaces, surface faceting, segregation and fracture, and electro-acoustical devices.[1] However, at the present time little is known about their dispersion relations. Model calculations that essentially neglect relaxation have been carried out on the alkali halide crystals by the groups of de Wette[2] in Austin, and Benedek[3] in Milan. Similar calculations for metals are only being started.[4] Because of their large penetration depths neutrons are not sensitive to surfaces while Brillouin light scattering and electron diffraction probe only surface phonons with very large wavelengths. The best tool for studying surface phonons is probably provided by the inelastic scattering of low-energy He atoms. They are scattered only by the first monolayer and their wavelength (≈1 Å) is comparable to lattice dimensions so that the entire Brillouin zone is probed.

Recently we reported the first clearly resolved structures in time-of-flight spectra of low-energy He atoms from LiF crystals.[5] The same apparatus is used here. A nozzle beam is expanded from a pressure of 200 atm and a temperature of 80 °K through a 5-μm-diam nozzle to produce a beam of about 20-meV kinetic energy with a velocity halfwidth of $\Delta v/v \lesssim 1\%$ [full width at half maximum (FWHM)].[5-7] After collimation to an angular spread of 0.30° (FWHM) the beam is chopped into pulses of 9 μsec and strikes the LiF target at 75.6 cm from the chopper. The freshly cleaved LiF was baked as described by Estel *et al.*[8] and after treatment produced sharp diffraction and selective adsorption[9] features indicating a clean well-ordered surface. The fixed detector is mounted at 90° to the incident beam at a distance of 101.5 cm from the target. Several improvements have recently been made: A commercial manipulator now allows an optimal adjustment of the angle of target rotation as well as cooling of the crystal to 133 °K. A homemade, extremely sensitive magnetic mass spectrometer[10] in an improved vacuum leads to a significant reduction in background and measuring time.

Figure 1 shows a typical time-of-flight spectrum taken at large incident angles $\theta_i = 64.2°$ near the $(\bar{1},\bar{1})$ diffraction peak. Note that the background is only about 15% of the greatest peak, whereas previously it was 70%. Six peaks are

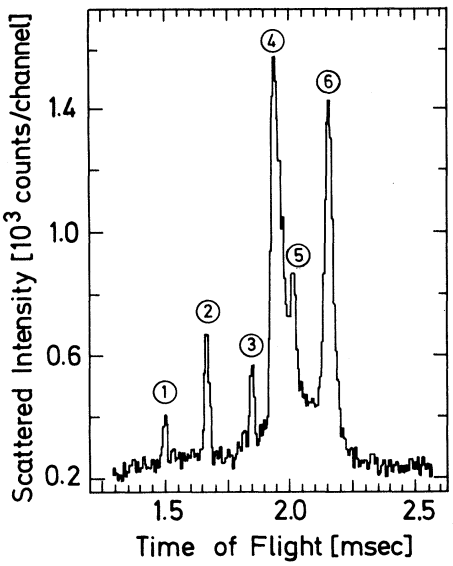

FIG. 1. Time-of-flight spectrum for He atoms scattered from a LiF(001) crystal at 300 °K along the ⟨100⟩ azimuth at $\theta_i = 64.2°$. The incident wave vector is 6.06 Å^{-1}. The channel width is 6.9 μsec and the total measuring time 1.0 h. Peak (3) is for elastic scattering from the nearest diffraction peak which is at $\theta_i = 66.4°$.

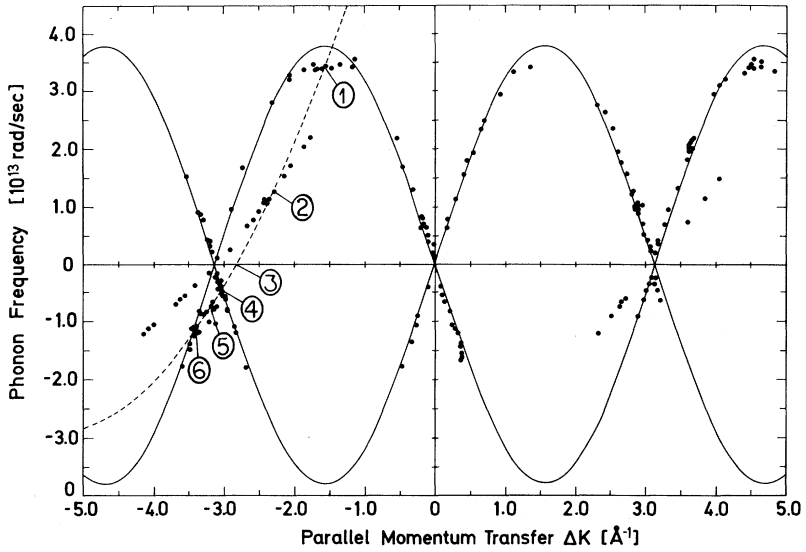

FIG. 2. Extended zone plot of measured values of phonon frequency and parallel momentum transfer. Solid line curves show the theoretical Rayleigh-phonon dispersion curves. The dashed line illustrates, with the example of the time-of-flight spectrum of Fig. 1 measured at $\theta_i = 62.4°$, how the time-of-flight maxima taken at one scattering angle relate to the dispersion curves.

clearly resolved at about (1), 1.50 msec; (2), 1.66 msec; (3), 1.85 msec; (4), 1.94 msec; (5), 2.01 msec; and (6), 2.15 msec. The peak (3) is attributed to a small amount of elastic scattering from the nearest $(\bar{1},\bar{1})$ diffraction peak at $\theta_i = 66.4°$. It is probably due to surface irregularities. The other peaks at greater flight times are due to creation events and the ones at shorter flight times are due to annihilation events. As discussed previously,[5] the frequency and wave vector of the single phonon causing each peak can be determined via conservation of energy and momentum from the scattering angle and flight time of the peak. This is illustrated in Fig. 2, which shows the scan curve for the spectrum of Fig. 1 and identifies the points on the extended zone diagram corresponding to the six peaks. The solid line shows the approximate locations of theoretical Rayleigh dispersion curves. With Fig. 2 the origin of the other maxima in Fig. 1 can be identified. Peak (1) is due to annihilation of a Rayleigh phonon with large wave vector Q near the zone boundary, peak (2) is as yet unexplained (see discussion at the end of this Letter), and peak (4) is due to creation of a Rayleigh phonon with small Q. Peak (5) is probably due to a bulk phonon at the surface and peak (6) is due to creation of a Rayleigh phonon with intermediate Q. Note that the Rayleigh-phonon peak heights are roughly in decreasing order of their frequency. This is expected from the Bose statistics although a number of other factors, such as cross sections,[11] kinematical focusing,[12] and selective adsorption[9] also affect the intensities in a complicated way.

Figure 2 also summarizes the data from altogether fifty measurements taken at incident angles between $\theta_i = 20°$ and 70°. It is seen that the measurements probe all possible combinations of creation and annihilation with momentum transfer both parallel and antiparallel to the incoming beam. The measurements extend out to the edges of the zone boundaries. Creation events with energies greater than 20 meV are excluded by conservation of energy.

In Fig. 3 all the data of Fig. 2 are plotted in a reduced zone diagram and are compared with the latest theoretical dispersion curves.[2,13] Figure 3 shows that all the points fall into essentially three groups: Bulk phonons at the surface with small frequency and wave vector; single Rayleigh phonons over the entire range of Q; and anomalous events following a curve with about half the slope of the Rayleigh dispersion curve. Similar anomalous features have also been found with NaF.

The agreement of the Rayleigh mode with both theories is within the errors except at the zone boundary. Here the frequencies are most sensitive to the interatomic forces, since at the small

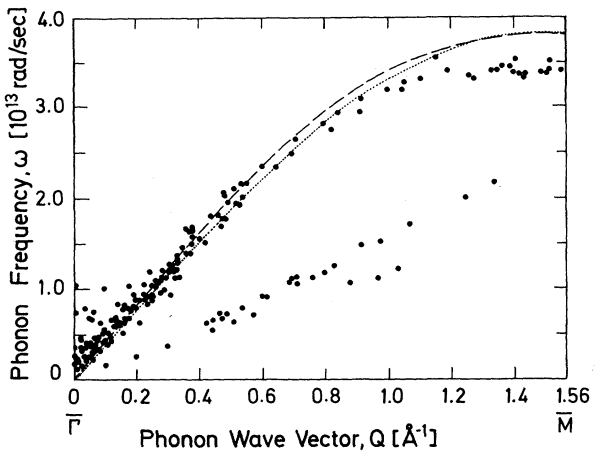

FIG. 3. Plot of all measured points in the irreducible section of the Brillouin zones for the ⟨100⟩ azimuth. The theoretical Rayleigh mode dispersion curves are shown by the dashed line, Chen, de Witte, and Alldredge (Ref. 2) and the dotted line, Benedek and Garcia (Ref. 13). The points well below the Rayleigh-phonon curve are discussed in the text.

wavelengths adjacent particles oscillate out of phase with respect to each other. Benedek and Garcia[13] attribute the reduced frequency to an increase of the polarizability of the more loosely held F atoms near the surface. de Wette[14] has suggested that the effect may be due to a number of opposing factors of which surface relaxation and a slight charge transfer should lead to a reduction in frequency.

The unidentified features do not appear to be a surface phonon dispersion curve since they occur only near the diffraction peaks and not near the specular peak. They are observed only when the momentum and energy transfer have the same sign (see Fig. 2). Moreover, the slope of the anomalous curve in NaF is nearly the same as in LiF although the surface phonon frequencies are distinctly different. A possible explanation for these events is presented elsewhere.[15]

We are extremely grateful to G. Benedek for many extensive and fruitful discussions. We also thank B. Feuerbacher and F. de Wette for their instructive comments. One of us (R.B.D.) thanks the Deutscher Akademischer Austauschdienst for a stipend.

[1]G. Benedek and G. Boato, Europhysics News 8 (No. 4), 5–8 (1977).

[2]T. S. Chen, F. W. de Wette, and G. P. Alldredge, Phys. Rev. B 15, 1167–1186 (1977).

[3]G. Benedek, Surf. Sci. 61, 603–634 (1976).

[4]V. Bortolani, F. Nizzoli, and G. Santoro, in *Proceedings of the International Conference on Lattice Dynamics, Paris, 1977*, edited by M. Balkanski (Flammarion, Paris, 1978), pp. 302–304.

[5]G. Brusdeylins, R. Bruce Doak, and J. Peter Toennies, Phys. Rev. Lett. 44, 1417–1420 (1980).

[6]J. P. Toennies and K. Winkelmann, J. Chem. Phys. 66, 3965–3979 (1977).

[7]G. B. Brusdeylins, H.-D. Meyer, J. P. Toennies, and K. Winkelmann, Prog. Astronaut. Aeronaut. 51, 1047–1059 (1977).

[8]J. Estel, H. Hoinkes, H. Kaarmany, H. Nahr, and H. Wilsch, Surf. Sci. 54, 393–418 (1976).

[9]G. Brusdeylins, R. Bruce Doak, and J. Peter Toennies, to be published.

[10]J. P. Toennies, W. Welz, and G. Wolf, J. Chem. Phys. 71, 614–642 (1979).

[11]G. Benedek and G. Seriani, J. Appl. Phys. Jpn., Suppl. 2, pt. 2, 545–548 (1974), Proceedings of the Second International Conference on Solid Surfaces, Japan, 1974.

[12]G. Benedek, Phys. Rev. Lett. 35, 234–237 (1975).

[13]G. Benedek and N. Garcia, Proceedings of the Fourth International Conference on Solid Surfaces, Cannes, 1980 (to be published), and private communication.

[14]F. de Wette, private communication.

[15]G. Benedek *et al.*, to be published.